Engineering Structures 300 (2024) 117174

Contents lists available at ScienceDirect

Engineering Structures

journal homepage: www.elsevier.com/locate/engstruct

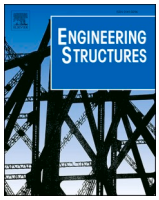

Computer-aided dynamic structural optimization using an advanced swarm algorithm

Vahid Goodarzimehr [a], Siamak Talatahari [b,c], Saeed Shojaee [a], Amir H. Gandomi [b,d,*]

[a] Shahid Bahonar University of Kerman, Department of Civil Engineering, Kerman, Iran
[b] Faculty of Engineering and Information Technology, University of Technology Sydney, Ultimo, NSW 2007, Australia
[c] Department of Civil Engineering, University of Tabriz, Tabriz, Iran
[d] University Research and Innovation Center (EKIK), Óbuda University, Budapest 1034, Hungary

ARTICLE INFO

Keywords:
Improved Marine Predators Algorithm (IMPA)
Dynamic constraint
Truss structure
Metaheuristic
Soft computing
Natural frequency

ABSTRACT

Natural frequencies, which are relatively easy parameters to obtain, provide efficient information about the dynamic behavior of structures. Controlling these parameters can help to minimize the destructive effect of dynamic loads on structures. However, the optimal design of the size and shape of truss structures with controlling dynamic constraints is an expensive problem. While frequency constraints are nonlinear and non-convex, handling natural frequencies as constraints is a challenging task, which prevents the phenomenon of resonance, large deformations, and destruction of a structure. Also, reducing the vibration amplitude of a structure would reduce the stress and deflections. In this paper, the Improved Marine Predators Algorithm (IMPA) is proposed and implemented for size and shape optimization of truss structures subject to natural frequency constraints. In this method, a Novel CF (NCF) factor is introduced to control the predator's step size when looking for prey. To evaluate the performance of IMPA, the optimum weight of structures under dynamic constraints was computationally investigated. To demonstrate the efficiency and robustness of IMPA, 37-bar truss bridge, 52-bar dome, 72-bar space truss, 120-bar dome, 200-bar planar truss, and 600-bar dome truss were optimized. Compared to other state-of-the-art algorithms, the results indicate that IMPA performs better in solving these nonlinear structural optimization problems.

1. Introduction

Most optimization problems fall into the category of nonlinear programming problems due to the nonlinearity of the variables [1]. Therefore, finding a suitable solution for them is a difficult task. One challenge in solving these problems is the existence of several local optimal answers. A local minimum point gives a smaller value for the objective function compared to its adjacent points, but it is not the global minimum point. Therefore, achieving a global optimal answer (or near it) in nonlinear problems is controversial, and the optimization process in many cases converges to the local minimum points. In general, optimization methods are categorized into two types: deterministic and stochastic techniques [2]. Stochastic methods utilize arbitrary sampling in their search space, whereas deterministic methods stop as soon as they reach the first local optimal point, which they cannot leave and proceed to another optimal point. Consequently, studies on algorithms that can escape from optimal local points have been conducted for a long time, and different methods have been proposed to date. However, stochastic algorithms have received more attention due to their simplicity and, therefore, ease of implementation using a computer. In the pursuit of finding optimal points, two crucial factors must be simultaneously considered. First, the optimization process encompasses the entirety of the search space, implying that the optimal solution can be located at any point within this domain. Second, adhering to a local strategy, the probability of discovering a new point that enhances the function's value is higher when it is closer to a point with a superior objective value rather than one with a poorer objective value [3].

Over the past five years, metaheuristic algorithms have become one of the most important and popular optimization methods, many of which have been developed for solving difficult problems. Due to their simplicity and flexibility, they can solve a variety of linear, nonlinear, constrained, and non-constrained problems. For instance, Goodarzimehr et al. [4] developed SRS to solve structural and mechanical problems. They organized a large comparative study and selected the

* Corresponding author at: Faculty of Engineering and Information Technology, University of Technology Sydney, Ultimo, NSW 2007, Australia.
E-mail address: gandomi@uts.edu.au (A.H. Gandomi).

https://doi.org/10.1016/j.engstruct.2023.117174
Received 20 April 2023; Received in revised form 30 October 2023; Accepted 12 November 2023
Available online 26 November 2023

best algorithm using Friedman's statistical test. Grzywiński [5] proposed a novel method called the Jaya algorithm, which was used to optimize the braced domes under frequency constraints. Dastan et al. [6] optimized steel frames utilized a hybrid method based on teaching-learning-based optimization (TLBO) and Charged System Search (CSS) algorithms. Talatahari et al. [7] proposed a multi-stage particle swarm for optimization of truss structures. Refs [8,9] provided a comprehensive framework for the application of metaheuristic algorithms in structural optimization. Tejani et al. [10] developed a multi-objective modified adaptive Symbiotic Organisms Search (SOS) with two modified phases planned along with a normal line method as an archiving technique for designing structures. Dehghani et al. [11] presented a modified Adolescent Identity Search Algorithm (AISA) for solving nonlinear frame structures. Faramarzi et al. [12] developed the Marine Predators Algorithm (MPA) for solving various optimization problems.

The metaheuristic algorithms mentioned above offer a range of good features, such as escape from the local optimal, low computation time, no need for specific information about the problem, high convergence rate, and simplicity. However, per the No Free Lunch theory [13], there are no metaheuristics that can address all types of problems. According to this point, researchers have used the idea of hybridization and development to solve this problem. For example, Li et al. [14] used BIM and hybrid metaheuristic algorithms for solving steel reinforcement problems. Dillen et al. [15] employed a hybrid gradient algorithm for the optimization of size, shape, and topology for steel structures. Ho et al. [16] proposed a new approach using MPA to train neural networks and then diagnose damages of three structural problems. Yousri et al. [17] developed a novel hybrid algorithm based on MPA. Houssein et al. [18] applied the reinforcement learning method to improve the efficiency of MPA for energy problems. Yousri et al. [19] proposed a new hybrid method to obtain the optimal parameters of the equivalent capacitance of the supercapacitor, an improved metaheuristic method using the Comprehensive Learning MPA. Elaziz et al. [20] proposed a new hybrid method using MPA and quantum theory to solve the problem of multilevel image grouping.

Structural optimization under natural frequency constraints is a difficult problem to handle. Since natural frequencies are a suitable framework for studying the dynamic behavior of trusses, controlling these parameters can help to reduce the dynamic effect of structures. However, optimizing the weight of structures subject to natural frequency constraints is a complex problem due to its nonlinear behavior. Therefore, the application of deterministic methods in optimizing these problems is challenging and even impossible in some cases. Hence, the use of a metaheuristic optimization method for solving these problems seems avoidable. Miguel [21] proposed a new hybrid method based on Harmony Search (HS) and Firefly Algorithm (FA) to optimize truss weight under frequency constraints. In the work by Lin et al. [22], a two-factor α-β algorithm based on the Cohen-Tucker criterion was proposed to optimize the mass of structures under frequency constraint. Wang et al. [23] presented an optimality criteria method to optimize truss structures under dynamic constraints. Gomes [26] developed a modified Particle Swarm Optimization (PSO) algorithm for vibration control and weight optimization of trusses. Kaveh and Mahdavi [27] developed a Colliding-Bodies algorithm (CBA) to optimize truss structures under frequency constraints, and several benchmark structures were optimized to demonstrate the effectiveness of the algorithm. Kaveh and Zolghadr [28] proposed a democratic version of PSO to prevent optimal local convergence and then optimized several structures under dynamic constraints. Farshchin et al. [29] developed a multi-class learning-based approach (MC-TLBO) for optimization, in which developing the learning process from one class to multiple classes increases the chance of finding better optimal answers. Five structures were optimized under frequency constraints to exhibit the algorithm's performance. Tejani et al. [32] developed three new versions of SOS. To exhibit the efficiency of the new algorithm, they optimized six trusses subject to dynamic constraints. Khatibinia and Naseralavi [33] introduced an efficient optimization algorithm to solve frequency constraint problems and also developed the orthogonal multi-gravitational Search Algorithm (GSA) as a new and effective method for optimization goals. By adding memory to the CBO, Kaveh and Mahdavi [34] created a balance between exploitation and exploration and introduced a new optimization technique. Mortazavi [35] proposed a new interactive fuzzy search algorithm version. Goodarzimehr et al. [37] introduced a novel formulation for weight and improved Chaos Game Optimization (CGO) for the optimum design of structures under dynamic constraints. Truong et al. [38] proposed a new fuzzy-based adaptive algorithm for solving frequency-constrained nonlinear dynamic problems, which performed better than other previous methods. Kaveh et al. [39] created an Improved Forensic-Based Examination (EFBI) for the ideal plan of frequency-constrained dome-like trusses, in which the Forensic-Based Examination calculation is a recently created population-based metaheuristic motivated by criminal examination preparation. Degertekin et al. [40] introduced the Parameter-Free Jaya Algorithm (PFJA) for evaluating and optimizing truss structures, considering inherent geometric constraints. PFJA stands out for its unique characteristic: it avoids both algorithm-specific and common parameters during the search process. Employing an elitist strategy, PFJA performs critical evaluations only when necessary and adaptively adjusts the population size throughout the optimization process. The efficacy of PFJA was demonstrated through the resolution of eight classical truss weight minimization problems, encompassing up to 59 design variables. Dastan et al. [41] proposed a hybrid TLBO-based CSS for optimization of steel frames. Kaveh et al. [42] developed another new algorithm to optimize the weight of truss structures under frequency constraints. They found that the classical Slime Mould Algorithm (SMA) suffers from slow convergence and often converges prematurely to non-optimal solutions, especially for large-scale optimization problems.

This presented study developed an effective method called the Improved Marine Hunter Algorithm (IMPA) to optimize the size and shape of five trusses under natural frequency constraints. MPA is inspired by the movement behaviors of marine predators when trapping prey in the ocean. The predator search behavior and strategy are based on Lévy random flight and Brownian motion. Random walking is an arbitrary method to find the next position, which depends on the present position and the probability of getting to the next location. This optimization method has three main optimization stages due to the different predator and prey speeds, which are subsequently described. In Step 1, the prey is moving faster than the predator. In Step 2, the prey and predator are moving at about the same speed. In Step 3, the predator is moving faster than the prey. The main disadvantage of MPA in the second step is the lack of a suitable mechanism to control the step size of the predator. In the main MPA, the CF factor is used to control the size of the moving steps. The CF factor decreases from one to zero, descending at each step. Since in the second step the predator moves towards the prey with a very small number of steps, applying the CF factor causes a further reduction in the size of the moving step. This makes the MPA spend more time exploring the local optimal. In this research, the NCF factor is proposed to control the size of moving steps. After the studies, we concluded that an equation should be proposed to accelerate the moving steps' size. The NCF factor helps IMPA to perform better than MPA. To evaluate the efficiency and robustness of IMPA, five real-world engineering problems under natural frequency constraints were optimized. The results show that IMPA is superior and more effective than other state-of-the-art metaheuristics.

2. Improved Marine Predators Algorithm (IMPA)

2.1. Marine Predators Algorithm (MPA)

The Marine Predators Algorithm (MPA), first proposed by Faramarzi et al. [12], is motivated by the behavior of marine predators to hunt

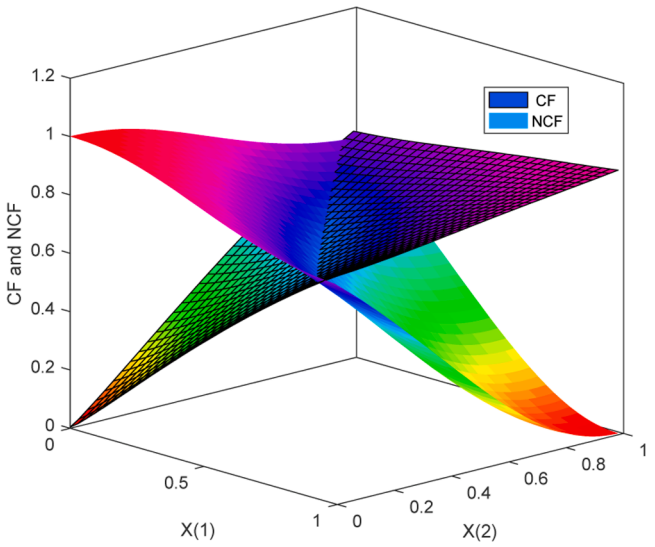

Fig. 1. 3D plot of CF and NCF.

Table 1
Definition of the optimization problem.

Objective function	$F(X) = \sum_{i=1}^{m} A_i \rho_i L_i$
Design variables	find $X = \{A, N\}$ where $A = \{A_1, A_2, A_3, ., A_m\}$ and $N = \{N_1, N_2, N_3, ., N_n\}$.
Constraints	$g_1(X): f_q \geq f_q^{\min}$ $g_2(X): f_r \leq f_r^{\max}$ $g_3(X): A_i^{\min} \leq A_i \leq A_i^{\max}$ $g_4(X): N_j^{\min} \leq N_j \leq N_j^{\max}$ where $i = 1, 2, ., m;\ j = 1, 2, ., n.$
Penalized	$F(X) = \begin{cases} \text{If there is no violation,} & F(X) \\ \text{otherwise,} & F(X) \times F_{Penalty} \end{cases}$

prey. Random movements can be modeled by two methods: Lévy flight and Brownian motion. These two methods are from the class of random walking methods. According to the theory of proper survival, predators should use the best movement method to increase the probability of hunting prey. In general, most animals use random walking techniques to find food in the wild. In the random walking system, selecting a new destination depends on the previous position and how to move to the new position. This plan of action is developed over a while and naturally selected by predators to keep them alive. One of the most popular random walk classes is Lévy flight, which has been utilized by many optimal search methods [43]. The class of these search plans relates to a development that is characterized by features, such as numerous small movements with longer movements, based on a specific probability distribution. Some studies show that the Lévy flight model is the preferred feeding mechanism followed by a considerable number of animals and sea creatures [43]. MPA selects a set of possible optimal solutions as the first test between low and high bounds, a process that is performed using Eq. (1):

$$X_0 = X_{\min} + rand(X_{\max} - X_{\min}) \tag{1}$$

where X_{min} and X_{max} are the minimum and maximum bounds of the search space, respectively; and rand is a uniform arbitrary vector *rand* ϵ [0,1].

The most suitable solution, which is considered the top predator, is defined by the matrix in Eq. (2), where each array contains information about the prey positions that are used in the search process:

$$Elite = \begin{bmatrix} X_{1,1}^1 & X_{1,2}^1 & \cdots & X_{1,d}^1 \\ X_{2,1}^1 & X_{2,2}^1 & \cdots & X_{2,d}^1 \\ \vdots & \vdots & \vdots & \vdots \\ \vdots & \vdots & \vdots & \vdots \\ X_{n,1}^1 & X_{n,2}^1 & \cdots & X_{n,d}^1 \end{bmatrix} \tag{2}$$

where X is the vector of the best solution; n is the number of possible solutions; and d is the number of variables. The predator's positions will be updated based on the prey matrix. The prey is defined using Eq. (3):

$$prey = \begin{bmatrix} X_{1,1} & X_{1,2} & \cdots & X_{1,d} \\ X_{2,1} & X_{2,2} & \cdots & X_{2,d} \\ \vdots & \vdots & \vdots & \vdots \\ \vdots & \vdots & \vdots & \vdots \\ X_{n,1} & X_{n,2} & \cdots & X_{n,d} \end{bmatrix} \tag{3}$$

where $X_{i,j}$ is the j^{th} dimension of the i^{th} solution. The MPA optimization mechanism is highly dependent on Eq. (2) and Eq. (3).

According to the differences in velocity between the predator and prey, the MPA process is divided into three main steps. In Step 1, the prey moves faster than the predator; in Step 2, the predator and prey move at the same velocities; and in Step 3, the predator moves faster than the prey. For each step, a specific iteration period is fixed. These stages are considered based on the laws governing the nature of the movement of the predator and prey in nature.

Step 1: The speed of the prey is greater than that of the predator. This step is implemented in the initial iterations of the optimization process. Execution of this step depends on the current iteration (*Iter*) and the maximum number of iterations (*MaxIter*). Eq. (4) is utilized when the *Iter* is less than one-third of *MaxIter*:

$$prey_i = prey_i + P.R \otimes (R_B \otimes (Elite_i - R_B \otimes prey_i)) \tag{4}$$

where P is a constant of value 0.5; R is an arbitrary value, $R \epsilon$ [0,1]; and R_B is an arbitrary vector based on the normal distribution that represents Brownian motion. Multiplying R_B in the prey simulates its motion.

Step 2: The prey and the predator are moving at almost the same velocity. This shows that each of them is looking for food. At this stage, both exploration and exploitation are important. This section runs in the middle part of the optimization process. The exploration and

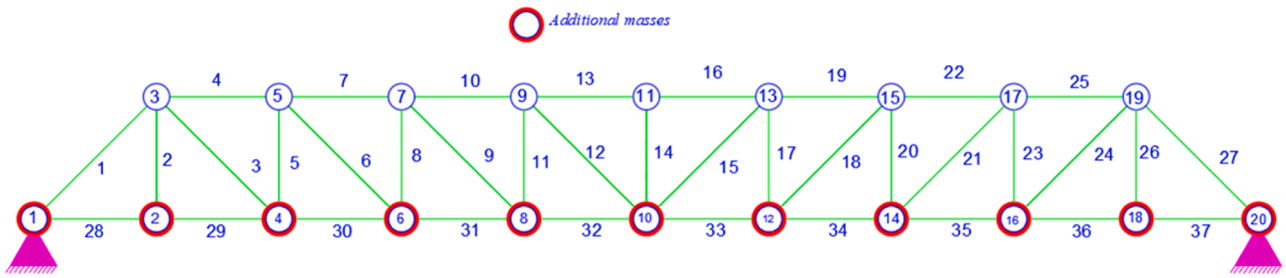

Fig. 2. The 37-bar bridge truss structure with additional masses.

Table 2
Comparative results of MPA, IMPA, and other methods for solving the 37-bar truss problem.

Design variables	OC [23]	GA [25]	PSO [26]	HS [21]	FA [21]	CBO [27]	DPSO [38]	TLBO [29]	TLBO [29]	SBO [30]	SOS [32]	SBO [30]	PFJA [40]	This study	
														MPA	IMPA
Y_3, Y_{19}	1.2086	1.1998	0.9637	0.8415	0.9392	0.9562	0.9482	0.9639	0.9830	0.9598	0.9598	0.9639	0.9724	1.0000	1.0052
Y_5, Y_{17}	1.5788	1.6553	1.3978	1.2409	1.3270	1.3236	1.3439	1.3551	1.3803	1.3289	1.3867	1.3551	1.3603	1.4255	1.3718
Y_7, Y_{15}	1.6719	1.9652	1.5929	1.4464	1.5063	1.5037	1.5043	1.5338	1.5645	1.5273	1.5698	1.5338	1.4976	1.5964	1.5624
Y_9, Y_{13}	1.7703	2.0737	1.8812	1.5334	1.6086	1.6318	1.6350	1.6367	1.6871	1.6727	1.6687	1.6367	1.6140	1.7039	1.6748
Y_{11}	1.8502	2.3050	2.0856	1.5971	1.6679	1.6987	1.7182	1.7052	1.7590	1.7509	1.7203	1.7052	1.6929	1.7555	1.7463
A_1, A_{27}	3.2508	2.8932	2.6797	3.2031	2.9838	2.7472	2.6208	2.9055	2.9913	2.9219	2.9038	2.9055	3.2214	3.9385	2.9154
A_2, A_{26}	1.2364	1.1201	1.1568	1.1107	1.1098	1.0132	1.0397	1.0012	1.0005	1.0007	1.0163	1.0012	1.0000	1.0383	1.0000
A_3, A_{24}	1.0000	1.0000	2.3476	1.1871	1.0091	1.0052	1.0464	1.0001	1.0042	1.0005	1.0033	1.0001	1.0000	1.0072	1.0000
A_4, A_{25}	2.5386	1.3655	1.7182	3.3281	2.5955	2.5054	2.7163	2.5598	2.5958	2.6633	3.1940	2.5598	2.6189	2.6114	2.5564
A_5, A_{23}	1.3714	1.5962	1.2751	1.4057	1.2610	1.1809	1.0252	1.2523	1.2139	1.2387	1.0109	1.2523	1.3890	1.3799	1.0373
A_6, A_{21}	1.3681	1.2642	1.4819	1.0883	1.1975	12603	1.5081	1.2141	1.1423	1.2030	1.5877	1.2141	1.5061	1.3722	1.2789
A_7, A_{22}	2.4290	1.8254	4.6850	2.1881	2.4264	2.7090	2.3750	2.3851	2.3170	2.4843	2.4104	2.3851	2.7945	2.5980	2.3844
A_8, A_{20}	1.6522	2.0009	1.1246	1.2223	1.3588	1.4023	1.4498	1.3881	1.5100	1.3706	1.3864	1.3881	1.5383	1.7561	1.4833
A_9, A_{18}	1.8257	1.9526	2.1214	1.7033	1.4771	1.4661	1.4499	1.5235	1.5172	1.4618	1.6276	1.5235	1.7091	1.0431	1.5233
A_{10}, A_{19}	2.3022	1.9705	3.8600	3.1885	2.5648	2.6107	2.5327	2.6065	2.2722	2.4432	2.3594	2.6065	2.6400	1.8654	2.5348
A_{11}, A_{17}	1.3103	1.8294	2.9817	1.0100	1.1295	1.1764	1.2358	1.1378	1.2112	1.2758	1.0293	1.1378	1.1418	1.2786	1.2550
A_{12}, A_{15}	1.4067	1.2358	1.2021	1.4074	1.3199	1.3767	1.3528	1.3078	1.2739	1.3491	1.3721	1.3078	1.3366	1.2021	1.2450
A_{13}, A_{16}	2.1896	1.4049	1.2563	2.8499	2.9217	2.8609	2.9144	2.6205	2.4934	2.3831	2.0673	2.6205	2.5320	2.1639	2.3555
A_{14}	1.0000	1.0000	3.3276	1.0269	1.0004	1.0064	1.0085	1.0003	1.0000	1.0000	1.0000	1.0003	1.0000	1.0267	1.0000
Best (kg)	366.50	368.84	377.20	361.50	360.05	359.92	360.40	359.88	359.96	359.88	360.86	359.88	363.05	362.120	359.985
Worst	-	-	-	-	-	-	-	-	-	-	-	-	-	369.586	360.213
Mean	NA	NA	381.20	362.04	360.37	360.44	362.21	360.80	360.83	360.23	364.85	360.80	363.93	365.170	360.107
SD	NA	9.0325	4.26	0.52	0.26	0.35	1.68	0.63	0.49	0.47	2.9650	0.633	0.5529	2.1700	0.0593
NFEs	NA	NA	12,500	20,000	5000	6000	6000	12,000	12,000	12,000	4000	12,000	5600	6000	6000

exploitation process is carried out simultaneously so that half of the population is used for exploration and the other half is utilized for exploitation. At this stage, the predator is in charge of exploitation, and the predator is in charge of exploration. Based on this theory, if the prey is moving with Lévy motion, the best strategy for the predator is Brownian motion. This process is performed using Eq. (5) when *Iter* is greater than one-third of *MaxIter* and less than two-thirds of *MaxIter*:

$$prey_i = prey_i + P.R \otimes (R_L \otimes (Elite_i - R_L \otimes prey_i)) \tag{5}$$

where RL is a vector of arbitrary numbers based on the Lévy distribution expressing Levy motion. Prey movement by the Lévy method is obtained by multiplying R_L and prey. Adding step size to the prey position simulates prey movement. This accelerates the operation because the size of the Lévy distribution stage is related to the small stages. This step is defined for the second half of the population by using Eq. (6):

$$prey_i = Elite_i + P.CF \otimes (R_B \otimes (R_B \otimes Elite_i - prey_i)) \tag{6}$$

The predator's motion is simulated by the Brownian method of multiplying R_B and Elite. Accordingly, the prey changes its location based on the movement of the predators in Brownian motion. *CF* is a parameter to control the size of the predator's movement steps, which is calculated as follows:

$$CF = \left(1 - \frac{Iter}{MaxIter}\right)^{\left(2 \times \frac{Iter}{MaxIter}\right)} \tag{7}$$

Step 3: The last step of MPA is related to maximum usability. When *Iter* is greater than two-thirds of *MaxIter*, the predator moves faster than the prey. Low-velocity ratios (v = 0.1) are the best strategy for the Lévy predator. This step is modeled using Eq. (8):

$$prey_i = Elite_i + P.CF \otimes (R_L \otimes (R_L \otimes Elite_i - prey_i)) \tag{8}$$

In Lévy's method, the predator's motion is obtained by multiplying RL by Elite. By adding step size to Elite, predator movements are modeled. The location of the prey is updated using this fitness. Environmental issues, such as vortex formation, or the effects of Fish Aggregating Devices (*FADs*) are other factors that change the behavior of marine predators (Filmalter et al., 2011 [44]). As an example, sharks spend more than 80% of their time looking for *FADs* and exploring different areas to find an environment with new prey for the other 20% of the time. *FADs* are local optimization operators whose job is to trap in the search space. The longer the duration of these movements, the higher the quality of optimization achieved. The process of *FADs* is defined using Eq. (9):

$$prey_i = \begin{cases} prey_i + CF[X_{\min} + R \otimes (X_{\max} - X_{\min})] \otimes U & if \quad r \le FADs \\ prey_i + [FADs(1-r) + r](prey_{r1} - prey_{r2}) & if \quad r > FADs \end{cases} \tag{9}$$

where *U* is the binary vector (i.e. 0, 1). $FADs = 0.2$ is the probability of *FADs'* effect. It is controlled with an arbitrary vector in [0,1], where if the array is less than 0.2, make it zero and 1 if it is bigger than (or equal to) 0.2. *r* is the uniform arbitrary number in [0,1]. X_{min} and X_{max} are the vectors with minimum and maximum bounds, respectively. In addition, r_1 and r_2 subscripts present arbitrary indices of the prey matrix.

Regarding the tuning these parameters, it's important to note that our proposed new IMPA does not introduce any additional parameters beyond the conventional MPA. Therefore, conducting extensive sensitivity analyses, while valuable in many cases, might not be necessary in our specific context. Additionally, the parameters shared with the classic MPA, such as P, R, RL, and RB, remain consistent with values used in previous research, enhancing the continuity of our approach.

2.2. Introducing a Novel CF (NCF)

The particle movement mechanism in MPA is based on a random walking strategy, in which the new position is sensitive to the current situation. Lévy and Brownian methods are employed for conducting search operations in numerous small steps. Proper use of Lévy and Brownian methods can provide better opportunities to search for optimal answers. Prey has the option to move using either Lévy or Brownian strategies. However, predators should avoid searching for prey using the Lévy method. In general, both the predator and prey use Lévy and Brownian with the same percentage during the search. However, the experience shows that for areas with low prey, the predator should use the Levy motion. In regions that are abundant with prey, predators are more effective when utilizing Brownian motion [43]. In summary, the predator should employ Lévy motion at low speeds regardless of the prey's movement strategy, be it Lévy or Brownian. When the prey moves at Lévy speeds, the predator adopts Brownian

Table 3
Natural frequencies (Hz) of the 37-bar bridge truss structure.

Natural frequency	OC [23]	GA [25]	PSO [26]	HS[21]	FA [21]	CBO [27]	DPSO [38]	TLBO [29]	TLBO [29]	SBO [30]	SOS [32]	SBO [30]	PFJA [40]	This study	
														MPA	IMPA
f_1	20.0850	20.0013	20.0001	20.0037	20.0024	20.0031	20.0194	20.0001	20.0001	20.0001	20.0366	20.0001	20.0027	20.0010	20.0010
f_2	42.0743	40.0305	40.0003	40.0050	40.0019	40.0060	40.0113	40.0005	40.0005	40.0000	40.0007	40.0000	20.0027	40.0020	40.0490
f_3	62.9383	60.0000	60.0001	60.0082	60.0043	60.0033	60.0082	60.0066	60.0066	60.0000	60.0138	60.0000	40.0016	60.0020	60.0020

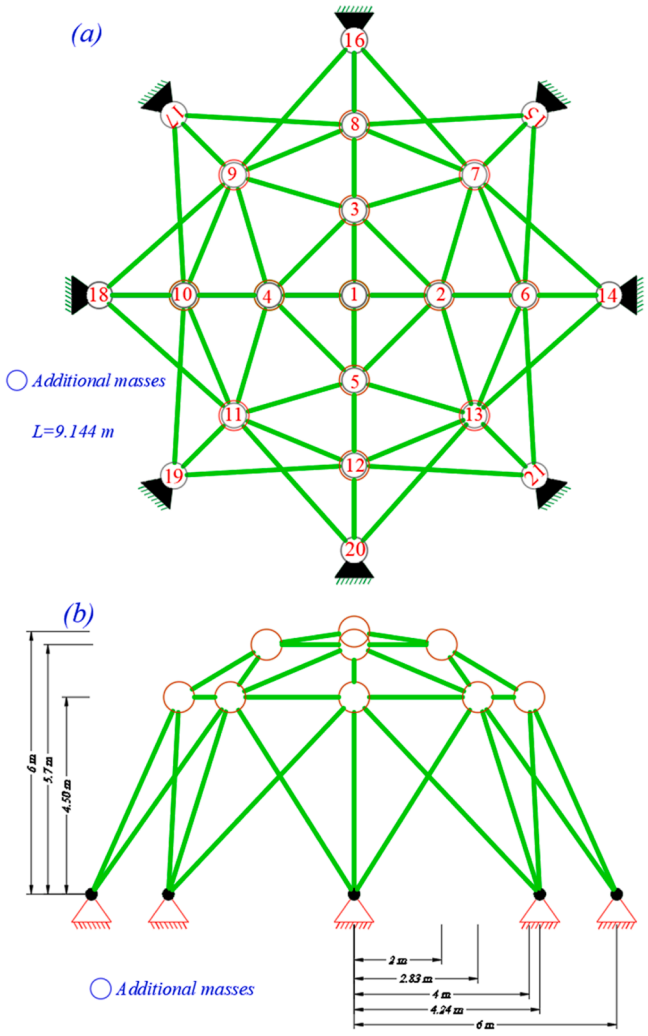

Fig. 3. The 52-bar space truss structure with additional masses: (a) top view; (b) side view.

motion. However, at high speeds, the predator remains stationary.

The main weakness of MPA is its second step or the so-called middle stage of the optimization process. This step occurs when exploration ends, and the exploitation phase begins. They move in the Brownian motion when the predator operation phase is activated. Due to the existence of many local optimizations, the new situation is sensitive to the current one. According to the fact that many steps are used to move to a new position, it is necessary to define a mechanism to control the size of the moving steps. The original MPA algorithm uses the CF factor (Eq. (7)) to fulfill this aim. The equation causes the predator to decrease Brownian motion in descending order in each iteration.

Based on experience, the CF factor does not control the step size of the MPA properly and spends more time in the area with local optimal. Therefore, introducing a new equation for CF can enhance the algorithm's performance. This study introduces the Novel CF (NCF) factor to control the size of predator movement steps. The CF factor is applied at the stage when the predator moves with the Brownian method (Eq. (6)) to direct the predator to an area with more prey. Therefore, a new equation that works in ascending order is needed to accelerate the search mechanism in this area.

The ascending exponential factor NCF in each iteration controls the size of the movement steps defined in Eq. (10). Fig. 1 presents a 3D plot comparing the CF and NCF coefficients.

Table 4
Comparative results of MPA, IMPA, and other methods for solving the 52-bar dome truss problem.

Design variables	Bi-factor [24]	NGHA [25]	PSO [26]	HS [21]	FA [21]	CSS-BBBC [31]	DPSO [28]	TLBO [29]	MC-TLBO [30]	SOS [32]	SBO [30]	PFJA [40]	This study	
													MPA	IMPA
Z_A	4.3201	5.8851	5.5344	4.7374	6.4332	5.3310	6.1123	6.0026	5.9531	5.7624	5.9644	60.0081	5.2232	5.2872
X_B	1.3153	1.7623	2.0885	1.5643	2.2208	2.1340	2.2343	2.2626	2.2908	2.3239	2.2834	2.5695	1.7915	2.3564
Z_B	4.1740	4.4091	3.9283	3.7413	3.9202	3.7190	3.8321	3.7452	3.7037	3.7379	3.7240	3.7000	3.7001	3.7119
X_F	2.9169	3.4406	4.0255	3.4882	4.0296	3.9350	4.0316	3.9854	3.9660	3.9842	3.9738	4.1590	3.6571	3.9948
Z_F	3.2676	3.1874	2.4575	2.6274	2.5200	2.5000	2.5036	2.5000	2.5001	2.5121	2.5000	2.5162	2.5263	2.5000
$A_1 - A_4$	1.00	1.0000	0.3696	1.0085	1.0050	1.0000	1.0001	1.0000	1.0002	1.0988	1.0000	1.0000	1.0144	1.0000
$A_5 - A_8$	1.33	2.1417	4.1912	1.4999	1.3823	1.3056	1.1397	1.1210	1.0962	1.0031	1.0933	1.6649	1.5378	1.0002
$A_9 - A_{16}$	1.58	1.4858	1.5123	1.3948	1.2295	1.4230	1.2263	1.2113	1.2252	1.1956	1.1893	1.0739	1.2636	1.2728
$A_{17} - A_{20}$	1.00	1.4018	1.5620	1.3462	1.2662	1.3851	1.3335	1.4486	1.4555	1.4563	1.4493	1.3957	1.6659	1.5005
$A_{21} - A_{28}$	1.71	1.9110	1.9154	1.6776	1.4478	1.4226	1.4161	1.4156	1.4172	1.3773	1.3883	1.3142	1.2698	1.3597
$A_{29} - A_{36}$	1.54	1.0109	1.1315	1.3704	1.0000	1.0000	1.0001	1.0000	1.0003	1.0055	1.0000	1.0000	1.0065	1.0000
$A_{37} - A_{44}$	2.65	1.4693	1.8233	1.4137	1.5728	1.5562	1.5750	1.5434	1.6204	1.7397	1.6055	1.3773	1.6682	1.5910
$A_{45} - A_{52}$	2.87	2.1411	1.0904	1.9378	1.4153	1.4485	1.4357	1.4034	1.3296	1.3084	1.3823	1.6690	1.5930	1.4446
Best (kg)	298.00	236.04	228.38	214.94	197.53	197.30	195.35	193.18	193.18	195.49	193.15	196.37	199.44	194.83
Worst	-	-	-	-	-	-	-	-	-	-	-	-	234.91	194.83
Mean	NA	NA	234.30	205.61	212.80	NA	198.71	200.30	197.87	214.66	195.94	198.44	209.80	194.83
SD	NA	37.462	5.22	12.44	17.98	NA	13.85	15.48	5.79	14.14	3.794	2.281	7.708	0.0015
NFEs	NA	NA	11,270	20,000	10,000	4000	6000	15,000	15,000	4000	15,000	5800	4000	4000

Table 5
Natural frequencies (Hz) of the 52-bar dome truss structure.

Natural frequency	Bi-factor [24]	NGHA [25]	PSO [26]	HS [21]	FA [21]	CSS-BBBC [31]	DPSO [28]	TLBO [29]	MC-TLBO [30]	SOS [32]	SBO [30]	PFJA [40]	This study	
													MPA	IMPA
f_1	15.22	12.81	12.75	12.22	11.31	12.98	11.31	11.46	11.59	12.71	11.61	14.1897	15.916	16.000
f_2	29.28	28.65	28.64	28.65	28.65	28.64	28.64	28.64	28.64	28.65	28.64	14.1897	28.648	28.648

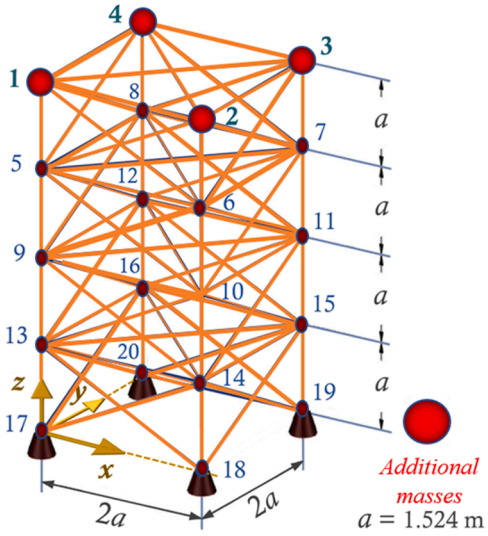

Fig. 4. The 72-bar space truss structure with additional masses.

$$\mathrm{NCF} = 1 - \frac{0.1}{1 + \exp\left(3 \times \frac{Iter}{MaxIter}\right)} \tag{10}$$

where *Iter* and *MaxIter* are the present iteration and the maximum number of iterations, respectively.

3. Definition of the optimization problem

In a typical optimization problem, an objective function, which is expressed in terms of single or multiple design variables, is a criterion for distinguishing the best answers from the pool of all possible answers. In other words, the optimal design is obtained by minimizing the objective function. While the main goal is to reduce costs, various other factors are important, and the relationships among these factors are highly complex. Considering a logical assumption, it can be inferred that reducing the weight of the structure also reduces the construction cost. Following this assumption, we selected the total weight of the structure, excluding lumped masses, as the objective function. Design variables include the nodal coordinates and cross-sectional areas of structural members. The mathematical definition of this problem is presented in Table 1.

In this table, A_i, ρ_i, and L_i are the cross-sectional area, density, and length of the i^{th} bar, respectively. N_j represents the nodal coordinates (in the directions x_j, y_j, and z_j) of the j^{th} node; and f_q and f_r are the q^{th} and r^{th} natural frequencies, respectively. Superscripts *max* and *min* denote the upper and lower allowable limits, respectively. A penalty condition is defined as follows: if there is no violation, the objective function will not be penalized; otherwise, it will be penalized using a penalty function defined as:

$$F_{Penalty} = (1 + \varepsilon_1 \times \psi)^{\varepsilon_2}, \psi = \sum \left(\psi_q + \psi_r\right), \tag{11}$$

$$\psi_q = \left|1 - \frac{\left|f_q - f_q^{\min}\right|}{f_q^{\min}}\right| \text{ and } \psi_r = \left|1 - \frac{\left|f_r - f_r^{\max}\right|}{f_r^{\max}}\right|, \tag{12}$$

where parameters ε_1 and ε_2 are constraint integers determined based on experience. A positive value greater than one is deemed appropriate for these parameters. Given the challenging nature of dynamic parameters, a high value for these penalty parameters appears necessary. Thus, we opted for a relatively high value (three) for these parameters according to Ref. [32] and [37]. It is important to note that while determining the precise value for these parameters could enhance the final results, our objective is to demonstrate that the core algorithm can yield satisfactory outcomes even without precisely determined penalty functions.

4. Structural design problems and discussions

A series of numerical examples concerning the optimization of truss

Table 6
Comparative results of MPA, IMPA, and other methods for solving the 72-bar space truss problem.

Design variables	CSS-BBBC [31]	CBO [27]	TLBO [29]	TLBO [29]	FA [21]	PSO [28]	SOS [32]	SBO [30]	PFJA [40]	This study	
										MPA	IMPA
$A_1 - A_4$ (cm^2)	2.854	3.3699	3.5491	3.4188	3.3411	2.9870	3.6957	3.4917	3.4933	2.28786	3.39204
$A_5 - A_{12}$ (cm^2)	8.301	7.3428	7.9676	7.9263	7.7587	7.8490	7.1779	7.9414	7.8400	6.41279	7.73949
$A_{13} - A_{16}$ (cm^2)	0.645	0.6468	0.6450	0.6450	0.6450	0.6450	0.6450	0.6450	0.6450	0.67155	0.65316
$A_{17} - A_{18}$ (cm^2)	0.645	0.6457	0.6450	0.6450	0.6450	0.6450	0.6569	0.6450	0.6450	0.66864	0.65134
$A_{19} - A_{22}$ (cm^2)	8.202	8.0056	8.1532	8.0143	9.0202	8.7650	7.7017	8.1154	7.9850	13.0587	8.17427
$A_{23} - A_{30}$ (cm^2)	7.043	8.0185	7.9667	7.9603	8.2567	8.1530	7.9509	8.0533	7.9650	8.64072	7.89357
$A_{31} - A_{34}$ (cm^2)	0.645	0.6458	0.6450	0.6450	0.6450	0.6450	0.6450	0.6450	0.6450	0.67751	0.64500
$A_{35} - A_{36}$ (cm^2)	0.645	0.6457	0.6450	0.6450	0.6450	0.6450	0.6450	0.6450	0.6450	1.92572	0.69367
$A_{37} - A_{40}$ (cm^2)	16.328	12.4585	12.9272	12.7903	12.045	13.450	12.3994	12.856	12.613	13.2702	12.8848
$A_{41} - A_{48}$ (cm^2)	8.299	8.1211	8.1226	8.1013	8.0401	8.0730	8.6121	8.0425	8.003	7.99027	8.14269
$A_{49} - A_{52}$ (cm^2)	0.645	0.6460	0.6452	0.6450	0.6450	0.6450	0.6450	0.6451	0.6450	0.69785	0.83189
$A_{53} - A_{54}$ (cm^2)	0.645	0.6459	0.6450	0.6473	0.6450	0.6450	0.6450	0.6450	0.6450	0.64560	0.66934
$A_{55} - A_{58}$ (cm^2)	15.048	17.3636	17.0524	17.4615	17.380	16.684	17.4827	17.213	17.051	15.3344	16.7582
$A_{59} - A_{66}$ (cm^2)	8.268	8.3371	8.0618	8.1304	8.0561	8.0561	8.1502	8.0804	8.054	9.29262	7.98835
$A_{67} - A_{70}$ (cm^2)	0.645	0.6460	0.6450	0.6450	0.6450	0.6450	0.6740	0.6450	0.6450	0.65623	0.64992
$A_{71} - A_{72}$ (cm^2)	0.645	0.6476	0.6450	0.6451	0.6450	0.6450	0.6550	0.6450	0.6450	0.67111	0.64500
Best (kg)	327.507	324.755	327.568	327.575	327.691	328.81	325.558	327.552	324.9563	336.888	325.195
Worst	-	-	-	-	-	-	-	-	-	430.548	327.210
Mean	NA	330.415	328.684	327.693	329.890	332.24	331.122	327.6797	325.297	379.995	325.923
SD	NA	7.7063	0.73	0.1250	2.59	4.23	4.227	0.0675	0.36	27.618	0.583
NFEs	4000	6000	15,000	15,000	10,000	42,840	4000	15,000	5360	6000	6000

Table 7
Natural frequencies (Hz) of the 72-bar space truss problem.

Natural frequency	CSS-BBBC [31]	CBO [27]	TLBO [29]	TLBO [29]	FA [21]	PSO [28]	SOS [32]	SBO [30]	PFJA [40]	This study	
										MPA	IMPA
$\mathbf{f_1}$	4.000	4.000	4.000	4.000	4.000	3.9999	4.0023	4.0000	4.0000	4.0000	4.0001
$\mathbf{f_2}$	6.004	6.000	6.000	6.000	6.000	3.9999	4.0020	4.0000	4.0000	4.0000	4.0001

structures was selected to investigate the capability of the suggested algorithms. More specifically, five truss structures were considered for testing the suggested algorithm, including 37-bar, 52-bar, 72-bar, 120-bar, and 200-bar trusses. To test the relative performance of the suggested algorithm, its solutions were compared with those obtained using conventional methods from the literature. Moreover, to analyze the results in more detail, standard deviation (SD) and number of function evaluations (NFE) were used as parameters to test the stability of the results and computational cost of calculations, respectively. Each problem was executed 20 times for accurate evaluation.

4.1. 37-bar bridge truss structure

The first numerical example is a 37-bar truss, which is illustrated in Fig. 2. The design variables include 14 cross-sectional and 5 nodal variables. Thus, size and shape optimization are considered simultaneously for this truss. The lower and upper allowable cross-sectional areas are 1 and 10 cm^2, respectively, while the lower and upper allowable node variables are 0.1 and 3 m, respectively. The coefficient of elasticity is 2.1e11 N/m^2, and the mass density is 7800 Kg/m^3. Also, the constraints on natural frequencies f_1, f_2, and f_3 are as follows: $f_1 \geq 20$, $f_2 \geq 40$, and $f_3 \geq 60$ Hz. The lumped mass that is neglected in the calculation of the objective function is $m = 10$ kg, which is applied to the lower nodes of the bridge. The lower chord is modeled with a rectangular cross-section with 4e-3 m^2.

In this problem, MPA and IMPA were examined by setting population size, maximum iterations, and NFEs to 30, 200, and 6000, respectively. The obtained solutions (i.e. design variables of best solutions, values of best, worst, mean, SD of mass, and NFEs) for 20 different runs are presented in Table 2. The first three natural frequencies of the best solution obtained for each of the metaheuristics are presented in Table 3. The best mass reported by OC, GA, PSO, HS, FA, CBO, DPSO, TLBO, MC-TLBO, SBO, SOS, MPA, SBO, PFJA, and IMPA is 366.50, 368.84, 377.20, 361.50, 360.05, 359.92, 360.40, 359.88, 359.96, 359.88, 360.865, 359.88, 363.05, 362.343, and 359.631 kg, respectively. It is observed that IMPA obtains better best mass for the 37-bar truss compared to MPA and other considered algorithms from the literature with no constraint violation. The SBO obtained a better weight with a slight improvement, but, IMPA is ten percent better than the SBO method for the SD value. The mean weight for MPA and IMPA are 365.170 and 360.107 kg, respectively. Moreover, IMPA reported the best mean weight among the other metaheuristics except for FA, CBO, TLBO, MC-TLBO, and SBO. However, it should be noted that NFEs used in MPA and IMPA are fairly small compared to these methods. The result table also presents that the SD of weight improves from 2.1700 to 0.0593 for MPA. The statistical experiment shows that IMPA is better than other algorithms.

4.2. 52-bar space truss structure

The 52-bar truss is considered an optimization problem to examine the relative performance of IMPA, as shown in Fig. 3. The design variables of this problem include 8 cross-sectional and 5 nodal variables. The minimum and maximum allowable cross-sectional areas are 0.0001 and 0.001 m^2, respectively. The allowable displacement of each node is $\pm$ 2 m along the vertical axis. The coefficient of elasticity is $E = 2.1 \times 10^{11} (N/m^2)$, and the mass density is $\rho = 7800$ (kg/m^3). Also, the constraints on natural frequencies f_1 and f_2 are as follows: $f_1 \leq 15.916$ Hz and $f_2 \geq 28.649$ Hz. The lumped mass that is neglected in the calculation of the objective function is $m = 50$ kg; this load is applied to the truss at all free nodes of the dome. As can be seen in Fig. 3b, the truss structure is symmetric about the vertical axis.

In this problem, we evaluated MPA and IMPA using a population size of 20, maximum iterations of 200, and a total of 4000 function evaluations (NFEs). The obtained solutions for 20 different runs are presented in Table 4. The first two natural frequencies of the best solution obtained

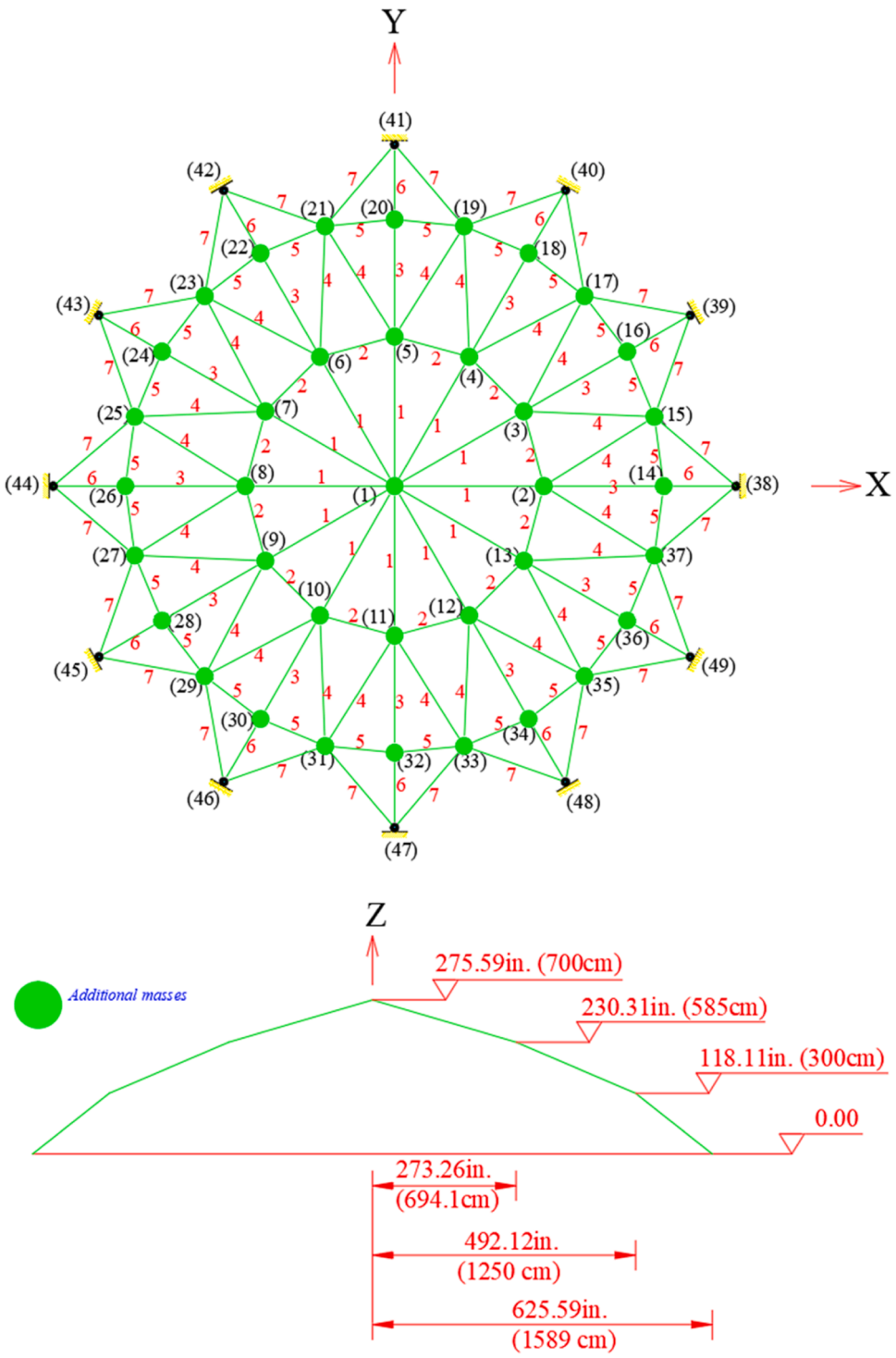

Fig. 5. The 120-bar dome structure with additional masses.

by the metaheuristics are tabulated in Table 5. The solutions indicate that the Bi-factor Algorithm, NGHA, PSO, HS, FA, CSS-BBBC, DPSO, TLBO, MC-TLBO, SOS, SBO, PFJA, MPA, and IMPA give trusses with optimum masses of 298.00, 236.04, 228.38, 214.94, 197.53, 197.30, 195.35, 195.49, 193.15, 196.37, 199.44, and 194.83 kg, respectively. Therefore, IMPA reduces mass by103.17, 41.21, 33.55, 20.11, 2.7, 2.47, 0.52, 0.66, and 4.61 kg compared to those obtained by Bi-factor Algorithm, NGHA, PSO, HS, FA, CSS-BBBC, DPSO, TLBO, MC-TLBO, SOS, and MPA, respectively. Additionally, IMPA finds better mass compared to MPA and other considered algorithms without any constraint violation. The best weight of SBO is 193.15 kg, which is better than IMPA. However, the SD for SBO is 3.794 and 0.0015 for IMPA. The mean mass obtained by PSO, HS, FA, DPSO, TLBO, MC-TLBO, SOS, MPA, and IMPA is 234.3, 205.61, 212.8, 198.71, 200.3, 197.87, 214.66, 209.80, and 194.83 kg, respectively. Therefore, IMPA reduces mean mass by39.47, 10.78, 17.97, 3.88, 5.47, 3.57, 19.83, 3.61, and 14.97 in comparison to those obtained from NGHA, HS, FA, DPSO, TLBO, SOS, PFJA, and MPA, respectively. The solutions specify that IMPA found the best mean mass weight among the other metaheuristics. Moreover, it should be noticed that NFEs used in MPA and IMPA are small in

Table 8
Comparative results of MPA, IMPA, and other methods for solving the 120-bar dome truss problem.

Design variables	PSO [28]	DPSO [28]	CSS [31]	CSS-BBBC [31]	CBO [42]	SOS [32]	SOS-ABF1 [32]	This study	
								MPA	IMPA
G_1 (cm^2)	23.494	19.607	21.710	17.478	19.691	19.520	19.544	19.5875	19.5049
G_2 (cm^2)	32.976	41.290	40.862	49.076	41.142	40.848	40.948	39.9528	40.3990
G_3 (cm^2)	11.492	11.136	9.048	12.365	11.155	10.322	10.448	10.6026	10.6130
G_4 (cm^2)	24.839	21.025	19.673	21.979	21.320	20.927	21.046	21.0688	21.1096
G_5 (cm^2)	9.964	10.060	8.336	11.190	9.833	9.655	9.504	9.94197	9.82206
G_6 (cm^2)	12.039	12.758	16.120	12.590	12.852	12.112	11.936	11.7284	11.7590
G_7 (cm^2)	14.249	15.414	18.976	13.585	15.160	15.0313	14.942	14.9355	14.8481
Best (kg)	9171.93	8890.48	9204.51	9046.34	8889.13	8713.30	8712.11	8707.904	8707.252
Worst	-	-	-	-	-	-	-	8725.562	8707.320
Mean	9251.84	8895.99	-	-	8891.25	8735.34	8727.42	8711.233	8707.278
SD	89.38	4.26	-	-	1.79	17.90	16.55	4.2348	0.0210
NFEs	6000	6000	4000	4000	6000	4000	4000	6000	6000

Table 9
Natural frequencies (Hz) of the 72-bar dome truss problem.

Natural frequency	PSO [28]	DPSO [28]	CSS [31]	CSS-BBBC [31]	CBO [42]	SOS [32]	SOS-ABF1 [32]	This study	
								MPA	IMPA
$\mathbf{f_1}$	9.000	9.000	9.002	9.000	9.000	9.000	9.001	9.000	9.000
$\mathbf{f_2}$	11.000	11.000	11.002	11.007	11.000	11.000	11.000	11.000	11.000
$\mathbf{f_3}$	11.005	11.005	11.006	11.018	11.000	11.000	11.000	11.000	11.000
$\mathbf{f_4}$	11.013	11.012	11.015	11.026	11.009	11.004	11.001	11.000	11.000
$\mathbf{f_5}$	11.042	11.047	11.045	11.048	11.049	11.071	11.067	11.000	11.000

comparison to PSO, HS, FA, DPSO, TLBO, SBO, PFJA, and MC-TLBO. Also, Table 4 shows that the SD of weight improved from 7.708 to 0.0015 for MPA.

4.3. 72-bar Space truss structure

A 72-bar truss was considered as the third problem, which is illustrated in Fig. 4. The design variables are cross-sectional areas that are divided into 16 sets. The minimum and maximum allowable cross-sectional areas are 0.645 and 30 cm^2, respectively. The coefficient of elasticity is $E = 6.98 \times 10^{11}(\mathrm{N/m^2})$, and the mass density is $\rho = 2770\ (\mathrm{kg/m^3})$. Also, the constraints on natural frequencies f_1 and f_2 are as follows: $f_1 \geq 4$ Hz and $f_2 \geq 6$ Hz. A lumped mass $m = 2770$ kg, which is neglected in the calculation of the objective function, is added to the truss at nodes 1–4.

For MPA and IMPA in this problem, we set the population size to 30, the maximum number of iterations to 200, and NFEs to 6000. The obtained solutions are presented in Table 6. The first two natural frequencies of the best results obtained for each metaheuristic are presented in Table 7. The best mass reported by CSS-BBBC, CBO, TLBO, MC-TLBO, FA, PSO, SOS, SBO, PFJA, MPA, and IMPA is 327.507, 327.568, 327.575, 327.691, 328.81, 325.558, 327.552, 324.9563, 336.88, and 325.195 kg, respectively. IMPA reduces weight by 2.312, 2.38, 2.496, 3.615, 0.363, 11.685, and 3.767 kg compared to CSS-BBBC, CBO, TLBO, MC-TLBO, FA, PSO, SOS, and MPA, respectively. It was observed that IMPA obtained the best result for the 72-bar truss compared to MPA and other considered algorithms from the literature with no constraint violation. The mean weight obtained for CBO, TLBO, MC-TLBO, FA, PSO, SOS, SBO, PFJA, MPA, and IMPA is 330.4154, 328.684, 327.693, 329.890, 332.24, 331.122, 327.6797, 325.297, 379.995, and 325.923 kg, respectively. The mean weight saving for IMPA is 4.4924, 2.761, 1.77, 3.967, 6.317, 5.199, 1.7567, and 54.072 compared to CBO, TLBO, MC-TLBO, FA, PSO, SOS, SBO, and MPA, respectively. Moreover, it should be noticed that NFEs used in MPA and IMPA are small in comparison to TLBO, MC-TLBO, FA, and PSO. Also, the results indicate that the SD of weight improved from 14.342 to 0.8280 for MPA.

4.4. 120-bar dome structure

A 120-bar truss, depicted in Fig. 5, was considered as another optimization problem to test the performance of IMPA. The truss bars are grouped based on z-axis symmetry. Thus, the design variables of this problem include 7 cross-sectional variables. The minimum and maximum allowable cross-sectional areas are 0.0001 and 0.01293 m^2, respectively. The coefficient of elasticity is $E = 2.1 \times 10^{11}(\mathrm{N/m^2})$, and the mass density is $\rho = 7971.81\ (kg\,m^3)$. Also, the constraints on natural frequencies f_1 and f_2 are $f_1 \leq 9$Hz and $f_2 \geq 11$Hz. The lumped masses, which are neglected in the calculation of the objective function, are 3000 kg at node-1, 500 kg at node-2 to node-13, and 100 kg at the rest of the free nodes.

Similar to the previous problem, 30, 200, and 6000 were considered for the population size, maximum iterations, and NFE for MPA and IMPA, respectively. Table 8 presents the final optimum results. The first five natural frequencies of the best solution observed for each of the metaheuristics are presented in Table 9. The best mass reported by PSO, DPSO, CSS, CSS-BBBC, CBO, SOS, SOS-ABF1, MPA, and IMPA are 9171.93, 8890.48, 9204.51, 9046.34, 8889.13, 8713.30, 8712.11, 8707.904, and 8707.252 kg, respectively. Therefore, IMPA reduces mean mass by464.678, 183.228, 497.258, 339.088, 181.878, 60.048, and 4.858 kg in comparison to those obtained from PSO, DPSO, CSS, CSS-BBBC, CBO, SOS, and SOS-ABF1, respectively. It is noted that IMPA gets the best mass in comparison to MPA and other considered algorithms from the literature with no constraint violation. The mean weight obtained for PSO, DPSO, CBO, SOS, SOS-ABF1, MPA, and IMPA is 9251.84, 8895.99, 8891.25, 8735.34, 8727.42, 8711.233, and 8707.278 kg, respectively. The mean mass saving for IMPA is 544.562, 188.712, 183.972, 28.062, 20.142, 3.955, and 25.729 compared to PSO, DPSO, CBO, SOS, SOS-ABF1, and MPA, respectively. The results indicate that IMPA reported the best mean mass among the considered algorithms. Also, Table 8 reveals that the SD of weight improved from 4.2348 to 0.0210 for MPA.

4.5. The 200-bar planar truss structure

This problem was presented in this study to examine the capabilities

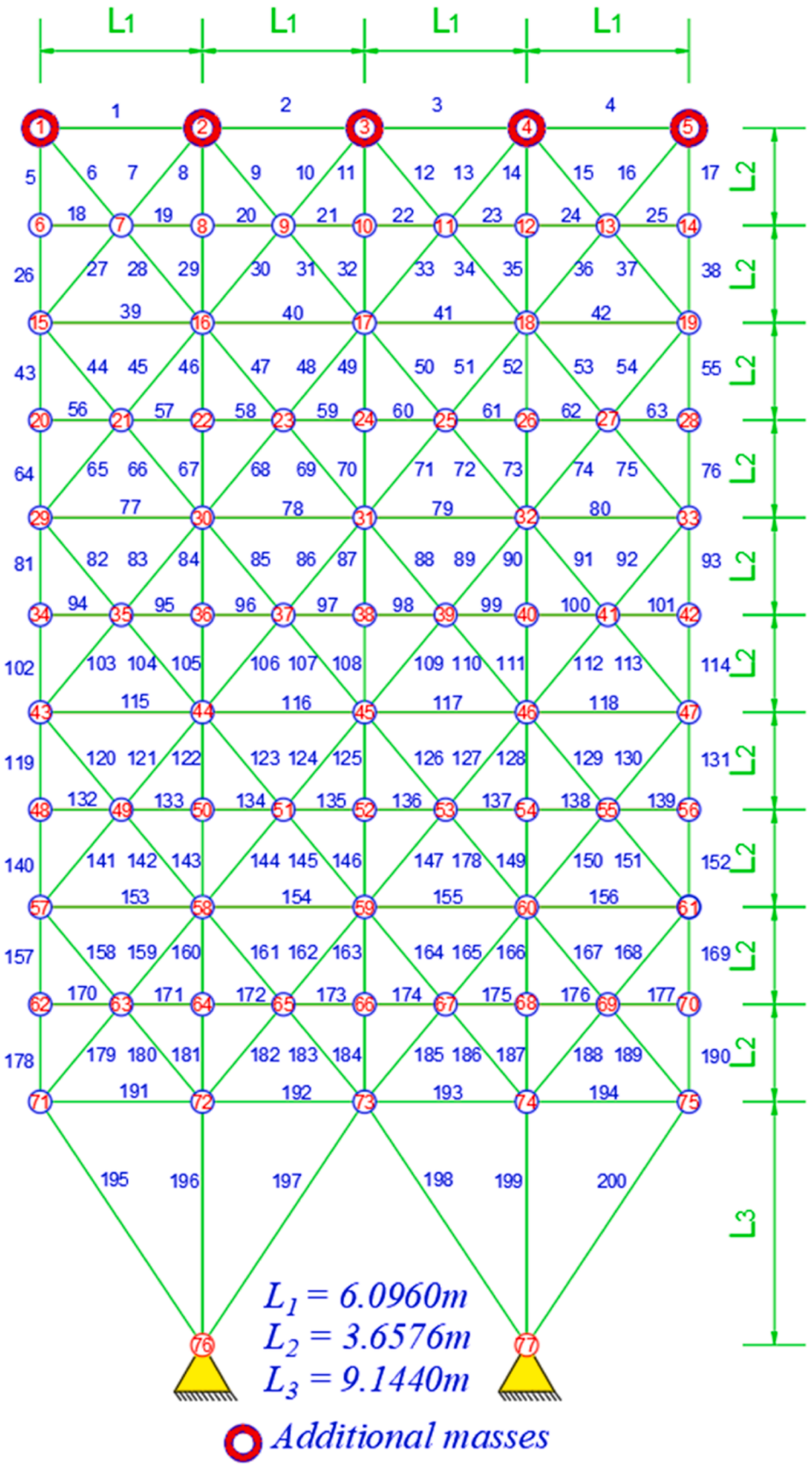

Fig. 6. The 200-bar planar truss structure with additional masses.

Table 10
Element grouping for the 200-bar truss structure.

Group	Element's number	Group	Element's number
G_1	A_1, A_2, A_3,A_4	G_{16}	A_{82}, A_{83}, A_{85}, A_{86}, A_{88},A_{89}, A_{91}, A_{92}, A_{103}, A_{104}, A_{106}, A_{107}, A_{109}, A_{110}, A_{112}, A_{113}
G_2	A_5, A_8, A_{11}, A_{14},A_{17}	G_{17}	A_{115}, A_{116}, A_{117}, A_{118}
G_3	A_{19}, A_{20}, A_{21}, A_{22}, A_{23},A_{24}	G_{18}	A_{119}, A_{122}, A_{125}, A_{128}, A_{131}
G_4	A_{18}, A_{25}, A_{56}, A_{63}, A_{94}, A_{101}, A_{132}, A_{139}, A_{170}, A_{177}	G_{19}	A_{133}, A_{134}, A_{135}, A_{136}, A_{137}, A_{138}
G_5	A_{26}, A_{29}, A_{32}, A_{35}, A_{38}	G_{20}	A_{140}, A_{143}, A_{146}, A_{149}, A_{152}
G_6	A_6, A_7, A_9,A_{10}, A_{12}, A_{13}, A_{15}, A_{16}, A_{27}, A_{28}, A_{30}, A_{31}, A_{33}, A_{34}, A_{36},A_{37}	G_{21}	A_{120}, A_{121}, A_{123}, A_{124}, A_{126}, A_{127}, A_{129},A_{130}, A141, A142, A_{44}, A_{145}, A_{147}, A_{148}, A_{150}, A_{151}
G_7	A_{39}, A_{40}, A_{41}, A_{42}	G_{22}	A_{153}, A_{154}, A_{155}, A_{156}
G_8	A_{43}, A_{46}, A_{49}, A_{52}, A_{55}	G_{23}	A_{157}, A_{160}, A_{163}, A_{166}, A_{169}
G_9	A_{57}, A_{58}, A_{59}, A_{60},A_{61}, A_{62}	G_{24}	A_{171}, A_{172}, A_{173}, A_{174}, A_{175}, A_{176}
G_{10}	A_{64}, A_{67}, A_{70}, A_{73}, A_{76}	G_{25}	A_{178}, A_{181}, A_{184}, A_{187}, A_{190}
G_{11}	A_{44}, A_{45}, A_{47}, A_{48}, A_{50}, A_{51}, A_{53}, A_{54}, A_{65}, A_{66}, A_{68}, A_{69}, A_{71}, A_{72}, A_{74}, A_{75}	G_{26}	A_{158}, A_{159}, A_{161},A_{162}, A_{164}, A_{165}, A_{167}, A_{168}, A_{179}, A_{180}, A_{182}, A_{183}, A_{185}, A_{186}, A_{188}, A_{189}
G_{12}	A_{77},A_{78}, A_{79}, A_{80}	G_{27}	A_{191}, A_{192}, A_{193}, A_{194}
G_{13}	A_{81}, A_{84}, A_{87}, A_{90}, A_{93}	G_{28}	A_{195}, A_{197}, A_{198}, A_{200}
G_{14}	A_{95},A_{96}, A_{97}, A_{98}, A_{99}, A_{100}	G_{29}	A_{196}, A_{199}
G_{15}	A_{102}, A_{105}, A_{108}, A_{111}, A_{114}		

of IMPA deals with a 200-bar truss, which is depicted in Fig. 6. The design variables are cross-sectional areas classified into 29 sets, as listed in Table 10, where the minimum and maximum allowable cross-sectional areas are 0.1 and 30 cm^2, respectively. The coefficient of elasticity is $E = 2.1 \times 10^{11}(\mathrm{N/m^2})$, and the mass density is$\rho = 7860\ (\mathrm{kg/m^3})$. The constraints on natural frequencies $f_1, f_2,$ and f_3 are as follows: $f_1 \geq 5$, $f_2 \geq 10$, and$f_3 \geq 15$ Hz. The lumped mass $m = 100\ kg$, which is neglected in the calculation of the objective function, is added to the top of the truss at nodes 1–5.

In this problem, MPA and IMPA were assessed with a population size of 50, maximum iterations of 200, and a total of 6000 function evaluations (NFE). The final results and the first three natural frequencies of the best solution obtained for each of the algorithms are presented in Tables 10 and 11, respectively. The best mass reported by OM-GSA, CBO, 2D-CBO, TLBO, MC-TLBO, CSS, PSO, SOS, SBO, PFJA, MPA, and IMPA is 2158.64, 2203.21, 2189.08, 2156.54, 2156.63, 2259.86, 3987.61, 2180.32, 2156.507, 2171.348, 2477.679, and 2168.697 kg, respectively. The weight saving for IMPA is 34.513, 20.383, 91.163, 1818.913, 11.623, and 308.982 kg compared to those obtained from CBO, 2D-CBO, CSS, PSO, SOS, and MPA, respectively. Moreover, it should be noticed that NFEs used in MPA and IMPA are small compared to those in OM-GSA, TLBO, MC-TLBO, and PSO. It is observed that IMPA obtained the best weight for the 200-bar truss compared to MPA and the other considered algorithms, except for SBO from the literature with no constraint violation. The mean weight obtained for OM-GSA, CBO, 2D-CBO, TLBO, MC-TLBO, PSO, SOS, MPA, and IMPA is 2189.58, 2481.49, 2308.44, 2157.54, 2157.44, 5027.78, 2303.30, 2727.117, and 2186.651 kg, respectively. The mean weight saving for IMPA is 2.929, 294.83, 121.789, 2841.129, 116.649, and 540.466 kg from OM-GSA, CBO, 2D-CBO, PSO, SOS, and MPA, respectively. Also, the results show that the SD of weight improved from 151.3996 to 9.9798 for MPA.

4.6. The 600-bar dome truss structure

The last example is a 600-bar dome truss structure, a large-scale problem with many design variables, which was considered for a more accurate evaluation of the proposed method. A 600-bar dome containing 216 nodes along with the side, top, and three-dimensional views are shown in Fig. 7. As the problem dimension increases, metaheuristic

Table 11
Comparative results of MPA, IMPA, and other methods for solving the 200-bar planar truss structure problem.

Design variables	OM-GSA [33]	CBO [34]	2D-CBO [34]	TLBO [29]	MC-TLBO[29]	CSS [35]	PSO [28]	SOS [32]	SBO [30]	PFJA [40]	This study	
											MPA	IMPA
G_1 (cm^2)	0.289	0.3268	0.4460	0.3030	0.3067	1.2439	2.4662	0.4781	0.3040	0.30785	1.114500	0.343205
G_2 (cm^2)	0.486	0.4502	0.4556	0.4479	0.4450	1.1438	0.1000	0.4481	0.4478	0.47168	0.478037	0.423233
G_3 (cm^2)	0.100	0.1000	0.1519	0.1001	0.1000	0.3769	0.1000	0.1049	0.1000	0.10020	0.214455	0.138624
G_4 (cm^2)	0.100	0.1000	0.1000	0.1000	0.1001	0.1494	0.1000	0.1045	0.1000	0.1001	0.645791	0.100421
G_5 (cm^2)	0.499	0.7125	0.4723	0.5124	0.5077	0.4835	0.1000	0.4875	0.5075	0.54175	1.572380	0.490236
G_6 (cm^2)	0.804	0.8029	0.7543	0.8205	0.8241	0.8103	2.8260	0.9353	0.8219	0.8184	0.799495	0.833291
G_7 (cm^2)	0.103	0.1028	0.1024	0.1000	0.1001	0.4364	0.1000	0.1200	0.1003	0.10096	0.653146	0.111904
G_8 (cm^2)	1.377	1.4877	1.4924	1.4499	1.4367	1.4554	4.6937	1.3236	1.4240	1.42367	2.853830	1.420440
G_9 (cm^2)	0.100	0.1000	0.1000	0.1001	0.1000	1.0103	0.1000	0.1015	0.1001	0.10006	0.100390	0.196390
G_{10} (cm^2)	1.554	1.0998	1.6060	1.5955	1.5787	2.1382	1.7291	1.4827	1.5929	1.63199	3.803280	1.640750
G_{11} (cm^2)	1.151	0.8766	1.2098	1.1556	1.1587	0.8583	1.8842	1.1384	1.1597	1.1373	1.636620	1.162110
G_{12} (cm^2)	0.131	0.1229	0.1061	0.1242	0.1000	1.2718	0.1000	0.1020	0.1275	0.10000	0.364709	0.104955
G_{13} (cm^2)	3.028	2.9058	3.0909	2.9753	2.9573	3.0807	3.7185	2.9943	2.9765	2.97378	2.827210	2.994990
G_{14} (cm^2)	0.101	0.1000	0.7916	0.1000	0.1000	0.2677	0.1000	0.1562	0.1001	0.10072	0.136978	0.316970
G_{15} (cm^2)	3.261	3.9952	3.6095	3.2553	3.2569	4.2403	2.3450	3.4330	3.2456	3.32736	3.205720	3.178240
G_{16} (cm^2)	1.612	1.7175	1.4999	1.5762	1.5733	2.0098	0.9164	1.6816	1.5818	1.5558	1.816720	1.657390
G_{17} (cm^2)	0.209	0.1000	0.1000	0.2680	0.2675	1.5956	0.1000	0.1026	0.2566	0.23602	0.146750	0.153994
G_{18} (cm^2)	5.020	5.9423	5.2951	5.0692	5.0867	6.2338	7.1603	5.0739	5.1118	5.20167	5.861840	5.041280
G_{19} (cm^2)	0.133	0.1102	0.1000	0.1000	0.1004	2.5793	30.000	0.1068	0.1001	0.10000	0.128989	0.207828
G_{20} (cm^2)	5.453	5.8959	4.5288	5.4281	5.4551	3.0520	6.1670	6.0176	5.4337	5.47313	5.494230	5.594130
G_{21} (cm^2)	2.113	2.1858	2.2178	2.0942	2.0998	1.8121	3.1906	2.0340	2.1016	2.0909	2.003670	2.093110
G_{22} (cm^2)	0.723	0.5249	0.7571	0.6985	0.7156	1.2986	0.2150	0.6595	0.6794	0.6673	1.101140	0.554408
G_{23} (cm^2)	7.724	7.2676	7.7999	7.6663	7.6425	5.8810	18.1871	6.9003	7.6581	7.53409	6.177600	7.513240
G_{24} (cm^2)	0.182	0.1278	0.3506	0.1008	0.1049	0.2324	0.1000	0.2020	0.1006	0.10489	1.798110	0.111828
G_{25} (cm^2)	7.971	7.8865	7.8943	7.9899	7.9352	7.7536	30.000	6.8356	7.9468	7.87075	12.35750	7.904840
G_{26} (cm^2)	2.996	2.8407	2.8097	2.8084	2.8262	2.6871	2.0233	2.6644	2.7835	2.81229	3.690740	2.804210
G_{27} (cm^2)	10.206	11.7849	10.4220	10.4661	10.4388	12.5094	16.061	12.1430	10.5277	10.7021	12.77270	10.51230
G_{28} (cm^2)	20.699	22.7014	21.2576	21.2466	21.2125	29.5704	30.000	22.2484	21.3027	21.75078	21.51770	21.50730
G_{29} (cm^2)	11.555	7.8840	11.9061	10.7340	10.8347	8.2910	30.000	8.9378	10.6207	10.44841	9.503500	10.44370
Best (kg)	2158.64	2203.21	2189.08	2156.54	2156.63	2259.86	3987.61	2180.32	2156.507	2171.348	2477.679	2168.697
Worst	-	-	-	-	-	-	-	-	-	-	3135.860	2209.204
Mean	2189.58	2481.49	2308.44	2157.54	2157.44	NA	5027.78	2303.30	2156.787	2171.573	2727.117	2186.651
SD	1.586	250.825	132.514	1.545	0.528	NA	708.95	83.589	0.211	0.2113	151.3996	9.9798
NFEs	15,000	10,000	10,000	23,000	23,000	10,000	20,000	10,000	23,000	10,546	10,000	10,000

Table 12
Comparative results of MPA and IMPA and other methods for solving the 200-bar planar truss structure problem.

No. frequency	OM-GSA [33]	CBO [34]	2D-CBO [34]	TLBO [29]	MC-TLBO[29]	CSS [35]	PSO [28]	SOS [32]	SBO [30]	PFJA [40]	This study	
											MPA	IMPA
$\mathbf{f_1}$	NA	5.0010	5.0016	5.0000	5.0000	5.0000	5.0650	5.0001	5.0000	5.0000	5.0000	5.0000
$\mathbf{f_2}$	NA	12.5247	13.3868	12.2171	12.2306	15.9610	13.1800	13.4306	12.2141	5.0000	16.5950	12.5880
$\mathbf{f_3}$	NA	15.1845	15.1981	15.0380	15.0259	16.4070	16.0970	15.2645	15.0191	12.3074	16.9440	15.0440

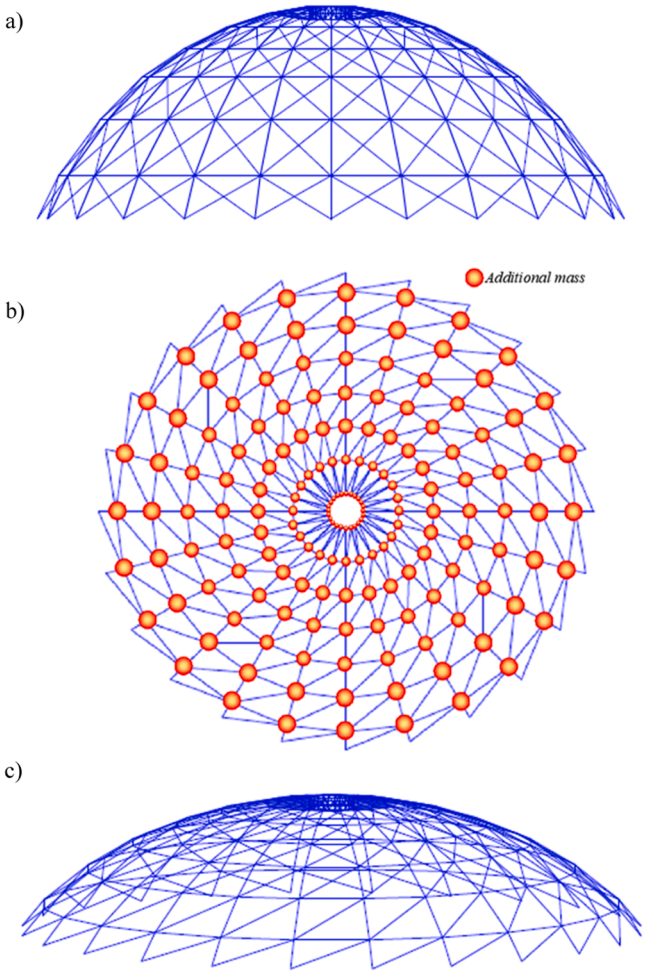

Fig. 7. The 600-bar dome: a) side view, b) top view, and c) 3D view.

Table 13
Comparative results of MPA, IMPA, and other methods for the 600-bar dome (**Case 1**).

Design variables	JA[5]	This study	
		MPA	IMPA
G_1 (cm^2)	12.7774	12.8901	12.52634
G_2 (cm^2)	5.13015	5.135249	5.109650
G_3 (cm^2)	11.8198	12.13155	11.67257
G_4 (cm^2)	6.63288	6.839473	6.606375
G_5 (cm^2)	8.12486	8.132936	8.092393
G_6 (cm^2)	1.75396	1.755703	1.646951
G_7 (cm^2)	16.2472	16.76335	16.18228
G_8 (cm^2)	16.2895	16.90569	16.22441
Best (kg)	8153.7646	8164.9541	8136.5213
Worst	-	8198.1752	8168.3269
Mean	8160.5211	8187.9823	8152.4241
SD	3.8249	5.2147	2.9812
NFEs	15,030	14,000	14,000
Run	10	20	20

Table 14
Comparative results of MPA and IMPA and other methods for the 600-bar dome (**Case 1**).

No. frequency	JA[5]	This study	
		MPA	IMPA
$\mathbf{f_1}$	5.0041	5.0052	5.0002
$\mathbf{f_2}$	5.0041	5.0052	5.0002
$\mathbf{f_3}$	7.0006	7.0031	7.0001
$\mathbf{f_4}$	7.0006	7.0031	7.0001
$\mathbf{f_5}$	7.0015	7.0045	7.0010

Table 15
Comparative results of MPA, IMPA, and other methods for the 600-bar dome (**Case 2**).

Design variables	[36]		JA[5]	This study	
	ECBO	COP		MPA	IMPA
G_1 (cm^2)	1.0299	1.0299	1.75176	1.018365	1.629701
G_2 (cm^2)	1.3664	1.3664	1.18111	1.351096	1.166237
G_3 (cm^2)	5.1095	5.1095	4.88782	5.052274	4.626269
G_4 (cm^2)	1.3011	1.3011	1.51622	1.286528	1.497127
G_5 (cm^2)	17.0572	17.0572	18.16588	16.86616	17.93712
G_6 (cm^2)	34.0764	34.0764	36.07637	33.69474	35.62207
G_7 (cm^2)	13.0985	13.0985	12.65709	12.95180	12.49770
G_8 (cm^2)	15.5882	15.5882	14.61127	15.41361	14.42727
G_9 (cm^2)	12.6889	12.6889	11.31977	12.54678	11.17722
G_{10} (cm^2)	10.3314	10.3314	8.45802	10.21569	8.351511
G_{11} (cm^2)	8.5313	8.5313	8.42854	8.435749	8.322402
G_{12} (cm^2)	9.8308	9.8308	9.73211	9.720695	9.609557
G_{13} (cm^2)	7.0101	7.010	7.29467	6.931587	7.202811
G_{14} (cm^2)	5.2917	5.2917	6.19220	5.232433	6.114224
G_{15} (cm^2)	6.2750	6.2750	6.43952	6.20472	6.358429
G_{16} (cm^2)	5.4305	5.4305	5.47595	5.369678	5.406993
G_{17} (cm^2)	3.6414	3.6414	3.26953	3.600616	3.228358
G_{18} (cm^2)	7.2827	7.2827	8.37244	7.201134	8.267009
G_{19} (cm^2)	4.4912	4.4912	4.49865	4.440899	4.442000
G_{20} (cm^2)	1.9275	1.9275	2.21967	1.905912	2.191718
G_{21} (cm^2)	4.6958	4.6958	4.61615	4.643207	4.558020
G_{22} (cm^2)	3.3595	3.3595	3.06674	3.321874	3.028122
G_{23} (cm^2)	1.7067	1.7067	1.85490	1.687585	1.831542
G_{24} (cm^2)	4.8372	4.8372	4.79602	4.783023	4.735625
G_{25} (cm^2)	2.0253	2.0253	1.60290	2.002617	1.582715
Best (kg)	6140.51	6140.51	6112.6438	6138.65	6109.93
Worst	-	-	-	6162.74	6118.25
Mean	6175.33	6175.33	6146.1936	6151.91	6114.09
SD	39.08	34.08	17.2355	19.320	12.870
NFEs	19,020	19,020	15,030	10,000	10,000
Run	5	5	10	20	20

Table 16
Comparative results of MPA and IMPA and other methods for the 600-bar dome (**Case 2**).

No. frequency	[36]		JA[5]	This study	
	ECBO	COP		MPA	IMPA
$\mathbf{f_1}$	5.002	5.001	5.0804	5.0210	5.0101
$\mathbf{f_2}$	5.003	5.001	5.0804	5.0210	5.0102
$\mathbf{f_3}$	7.001	7.001	7.0001	7.0001	7.0001
$\mathbf{f_4}$	7.001	7.001	7.0001	7.0001	7.0001
$\mathbf{f_5}$	7.002	7.002	7.0006	7.0030	7.0006

algorithms face challenges and may struggle to achieve the optimal solution. Therefore, it becomes crucial to propose an efficient method capable of optimizing large-scale problems effectively. Herein, two cases were considered. In case 1, all 600 design variables are divided into 8 groups. In case 2, all 600 design variables are divided into 25 groups. The results of the optimization of these two cases show how the convergence rate changes to the global optimal as the dimensions of the problem increase. The objective function is the summation of the weight of the structural elements. The modulus of elasticity and density are the same for all elements of the structure and equal to $E = 200\ GPa$ and $\gamma = 7850\ kg/m^3$, respectively. A non-structural mass of 100 kg is applied to all free nodes to obtain the structure's dynamic characteristics. However, this weight is not considered when calculating the objective function. An allowable cross-section of all members is selected between the upper and lower bounds of 1×10^{-4} and $100 \times 10^{-4}\ m^2$, respectively. The natural frequencies of the structure include $f_1 \geq 5$ and $f_3 \geq 7\ Hz$, which are considered design constraints.

The results of the 600-bar dome for cases 1 and 2 are presented in Tables 13 to 16. The best weight obtained by IMPA in the first case is 8136.5213, which is less than those obtained by JA. To calculate the standard deviation, the program was run 20 times, resulting in SD= 2.9812. A low SD value indicates good algorithm stability; in this study, IMPA exhibited greater stability compared to other methods. The results also show that IMPA performed better than the original MPA. Additionally, IMPA achieved superior values of SD, NFE, and BEST by IMPA compared to those obtained by MPA and JA. The results of frequencies one to five are presented in Table 14.

For a comparative analysis, the results of IMPA, Grzywiński et al., 2019 [5], and Kaveh and Ghazaan 2016 [36] are presented in Table 15. It can be observed that IMPA achieved a better answer than MPA and other methods. Specifically, ECDO achieved an optimal weight of 6140.51 with 19020 NFEs and SD = 39.08. COP reached the same optimal point with the same number of NFEs but with a lower standard deviation of 34.08. JA achieved the optimal answer of 6112.6438 with 15030 NFEs and SD= 17.2355, which performed better than ECDO and COP. In general, IMPA performed better than these state-of-the-art methods due to its ability to create a balance between exploitation and exploration. The results of frequencies one to five for the second case are presented in Table 16.

5. Conclusions

In this study, an improved version of MPA (IMPA) was proposed to optimize the weight and topology of trusses under natural frequency constraints. Over the last two years, researchers have applied MPA to solve different problems due to its good properties, such as a high convergence rate and good global search power. In the updated algorithm, the dominant behavior and strategy of the famous search and pursuit of marine predators have been modeled by Lévy flight and Brownian motion. According to the theory of proper survival, predators should use the best movement method to increase the probability of hunting prey. In general, most animals use random walking techniques to find food in the wild. These optimal movement techniques, which evolve based on the ecosystem, are naturally used by predators to trap prey. The family of such search strategies expresses a movement that is characterized by features like many small steps with longer movements, depending on a specific probability distribution. MPA consists of three stages. The main weakness of MPA is in the second stage, where the predator and prey move at the same velocity. Because the predator moves in small steps at this stage, they spend more time exploring the local optimal. The size of the movement steps is one of the most important factors that can improve the algorithm's performance if properly controlled. The original MPA method employed the CF factor to control the predator's step size. The CF factor is defined based on the number of iterations. Accordingly, the presented study proposed a new formula for controlling step size called NCF, which exponentially increases from zero to one. Herein, five real-world engineering problems with natural frequency constraints were optimized to evaluate IMPA's performance. However, optimization of the shape and size of the structures has not been addressed by previous researchers due to its complexity and nonlinearity. Therefore, by using the improved algorithm, a wide range of constrained and non-linear problems can be optimized, such as maximizing the axial force of laminated plates, minimizing the weight of concrete structures under the effect of gravity and dynamic loads, maximizing the buckling force of columns, and many others. For this purpose, it is necessary to define several parameters related to the problem, including the objective function, side constraints, internal constraints, generating a random population, and determining the stopping criterion (maximum repetition).

Author statement

In this paper, we developed a new advanced technique to find the optimum design of structures. In the revised version, we did our bests to address the comments provided by the respected reviewer which improved our work considerably. We hope the revision has improved the paper to a level of their satisfaction.

CRediT authorship contribution statement

Vahid Goodarzimehr: Conceptualization, Data curation, Formal analysis, Methodology, Visualization, Writing – original draft, Writing – review & editing. **Siamak Talatahari:** Conceptualization, Data curation, Methodology, Writing – review & editing. **Saeed Shojaee:** Methodology, Validation, Writing – original draft. **Amir H Gandomi**: Supervision, Writing - review & editing.

Declaration of Competing Interest

The authors declare that they have no known competing financial interests or personal relationships that could have appeared to influence the work reported in this paper.

Data Availability

No data was used for the research described in the article.

References

[1] Rao SS. Engineering Optimization: Theory and Practice. Wiley; 2009.
[2] Gandomi AH, She Yang X, Talatahari S, Alavi AH. Metaheuristic Applications in Structures and Infrastructures. Elsevier; 2013.
[3] Horst R, Tuy H. Global optimization: Deterministic approaches. Springer Science & Business Media; 2013.
[4] Goodarzimehr V, Talatahari S, Shojaee S, H.-Javaran S. Special relativity search for applied mechanics and engineering. Comput Methods Appl Mech Eng 2023;403 (Part A):115734.
[5] Grzywiński M, Dede T, Özdemir YI. Optimization of the braced dome structures by using Jaya algorithm with frequency constraints. Steel Compos Struct 2019;30(1): 47–55.
[6] Dastan M, Goodarzimehr V, Shojaee S, et al. Optimal design of planar steel frames using the hybrid teaching–learning and charged system search algorithm. Iran J Sci Technol Trans Civ Eng 2023. https://doi.org/10.1007/s40996-023-01124-8.
[7] Talatahari S, Kheirollahi M, Farahmandpour C, et al. A multi-stage particle swarm for optimum design of truss structures. Neural Comput Applic 2013;23:1297–309. https://doi.org/10.1007/s00521-012-1072-5.
[8] Kashani AR, Camp CV, Rostamian M, et al. Population-based optimization in structural engineering: a review. Artif Intell Rev 2022;55:345–452. https://doi.org/10.1007/s10462-021-10036-w.
[9] Sahab MGm, Toropov VV, Gandomi AH. 2 - A review on traditional and modern structural optimization: problems and techniques. Metaheuristic Appl Struct Infrastruct 2013:25–47. https://doi.org/10.1016/B978-0-12-398364-0.00002-4.
[10] Tejani GG, Pholdee N, Bureerat S, Prayogo D, Gandomi AH. Structural optimization using multi-objective modified adaptive symbiotic organisms search. Expert Syst Appl 2019;125:425–41. https://doi.org/10.1016/j.eswa.2019.01.068.
[11] Dehghani A, Goodarzimehr V, Shojaee S, Hamzehei Javaran S. Modified adolescent identity search algorithm for optimization of steel skeletal frame structures. Sci Iran 2023. https://doi.org/10.24200/sci.2023.60555.6868.

[12] Faramarzi A, Heidarinejad M, Mirjalili S, Gandomi AH. Marine predators algorithm: a nature-inspired metaheuristic. Expert Syst Appl 2020;152:113377.
[13] Wolpert DH, Macready WG. No free lunch theorems for optimization. IEEE Trans Evolut Comput 1997;1(1):67–82.
[14] Li M, Wong Billy CL, Liu Y, Chan CM, Gan Vincent JL, Cheng Jack CP. DfMA-oriented design optimization for steel reinforcement using BIM and hybrid metaheuristic algorithms. J Build Eng 2021;44:103310.
[15] Dillen W, Lombaert G, Schevenels M. A hybrid gradient-based/metaheuristic method for Eurocode-compliant size, shape and topology optimization of steel structures. Eng Struct 2021;239:112137.
[16] Ho LV, Nguyen DH, Mousavi M, Roeck GD, Bui-Tien T, Gandomi AH, Wahab MA. A hybrid computational intelligence approach for structural damage detection using marine predator algorithm and feedforward neural networks. Comput Struct 2021;252:106568.
[17] Yousri D, Fathy A, Rezk H. A new comprehensive learning marine predator algorithm for extracting the optimal parameters of supercapacitor model. J Energy Storage 2021;42:103035.
[18] Houssein EH, Ibrahim IE, Kharrich M, Kamel S. An improved marine predators algorithm for the optimal design of hybrid renewable energy systems. Eng Appl Artif Intell 2022;110:104722.
[19] Yousri D, Fathy A, Rezk H, Babu TS, Berber MR. A reliable approach for modeling the photovoltaic system under partial shading conditions using three diode model and hybrid marine predators-slime mould algorithm. Energy Convers Manag 24 2021;3114269.
[20] Elaziz MA, Mohammadi D, Oliva D, Salimifard K. Quantum marine predators algorithm for addressing multilevel image segmentation. Appl Soft Comput 2021; 110:107598.
[21] Miguel LFF. Shape and size optimization of truss structures considering dynamic constraints through modern metaheuristic algorithms. Expert Syst Appl 2012;39 (10):9458–67.
[22] Lin JH, Che WY, Yu YS. Structural optimization on geometrical configuration and element sizing with static and dynamic constraints. Comput Struct 1982;15: 507–15.
[23] Wang D, Zhang WH, Jiang JS. Truss optimization on shape and sizing with frequency constraints. AIAA J 2004;42(3):622–30.
[24] Lin JH, Che WY, Yu YS. Structural optimization on geometrical configuration and element sizing with static and dynamic constraints. Comput Struct 1982;15: 507–15.
[25] Wei L, Mei Z, Guangming W, Guang M. Truss optimization on shape and sizing with frequency constraints based on genetic algorithm. Comput Mech 2005;35: 361–8.
[26] Gomes HM. Truss optimization with dynamic constraints using a particle swarm algorithm. Expert Syst Appl 2011;38(1):957–68.
[27] Kaveh A, Mahdavi VR. Colliding-bodies optimization for truss optimization with multiple frequency constraints. J Comput Civ Eng 11 (GDOT 2005) 2014:1–10.
[28] Kaveh A, Zolghadr A. Democratic PSO for truss layout and size optimization with frequency constraints. Comput Struct 2014;130:10–21.
[29] Farshchin M, Camp CV, Maniat M. Multi-class teaching–learning-based optimization for truss design with frequency constraints. Eng Struct 2016;106: 355–69.
[30] Farshchin M, Camp CV, Maniat M. Optimal design of truss structures for size and shape with frequency constraints using a collaborative optimization strategy. Expert Syst Appl 2016;66:203–18.
[31] Kaveh A, Zolghadr A. Truss optimization with natural frequency constraints using a hybridized CSS-BBBC algorithm with trap recognition capability. Com- Put Struct 2012;102–103:14–27.
[32] Tejani GG, Savsani VJ, Patel VK. Adaptive symbiotic organisms search (SOS) algorithm for structural design optimization. J Comput Des Eng 2016;3(3):226–49.
[33] Khatibinia M, Naseralavi S. Truss optimization on shape and sizing with frequency constraints based on orthogonal multi-gravitational search algorithm. J Sound Vib 2014;333(24):6349–69.
[34] Kaveh A, Mahdavi VR. Two-Dimensional colliding bodies algorithm for optimal design of truss structures. Adv Eng Softw 2015;83:70–9.
[35] Mortazavi A. Size and layout optimization of truss structures with dynamic constraints using the interactive fuzzy search algorithm. Eng Optim 2021;53(3): 369391.
[36] Kaveh A, Ilchi M. Ghazaan, Optimal design of dome truss structures with dynamic frequency constraints. Struct Multidisc Optim 2016;53:605–21.
[37] Goodarzimehr V, Talatahari S, Shojaee S, H.-Javaran S, Sareh P. Structural design with dynamic constraints using weighted chaos game optimization. J Comput Des Eng 2022;9(6):2271–96.
[38] Truong D-N, Chou J-S. Fuzzy adaptive forensic-based investigation algorithm for optimizing frequency-constrained structural dome design. Math Comput Simul 2023;210:473–531.
[39] Kaveh A, Biabani Hamedani K, Kamalinejad M. An enhanced Forensic-Based Investigation algorithm and its application to optimal design of frequency-constrained dome structures. Comput Struct 2021;256:106643.
[40] Degertekin SO, Yalcin Bayar G, Lamberti L. Parameter free Jaya algorithm for truss sizing-layout optimization under natural frequency constraints. Comput Struct 2021;245:106461.
[41] Dastan M, Shojaee S, Hamzehei-Javaran S, Goodarzimehr V. Hybrid teaching–learning-based optimization for solving engineering and mathematical problems. J Braz. Soc. Mech. Sci. Eng 2022. https://doi.org/10.1007/s40430-022-03700-x.
[42] Kaveh A, Biabani Hamedani K, Kamalinejad M. Improved slime mould algorithm with elitist strategy and its application to structural optimization with natural frequency constraints. Comput Struct 2022;264:106760.
[43] Humphries NE, Queiroz N, Dyer JRM, Pade NG, Musyl MK, Schae fer KM. Environmental context explains Lévy and Brownian movement patterns of marine predators. Nature 2010;465(7301):1066.
[44] Filmalter JD, Dagorn L, Cowley PD, Taquet M. First descriptions of the behavior of silky sharks, Carcharhinus falciformis, around drifting fish aggregating devices in the Indian Ocean. Bull Mar Sci 2011;87(3):325–37.